Yrast structures in the neutron-deficient $^{127}_{59}Pr_{68}$ and $^{131}_{61}Pm_{70}$ nuclei

C. M. Parry,[1] A. J. Boston,[2] C. Chandler,[3] A. Galindo-Uribarri,[4] I. M. Hibbert,[1,*] V. P. Janzen,[4] D. T. Joss,[2] S. M. Mullins,[5] P. J. Nolan,[2] E. S. Paul,[2] P. H. Regan,[3] S. M. Vincent,[3] R. Wadsworth,[1] D. Ward,[4,†] and R. Wyss[6]

[1]*Department of Physics, University of York, Heslington, York, YO1 5DD, United Kingdom*
[2]*Oliver Lodge Laboratory, University of Liverpool, Liverpool, L69 3BX, United Kingdom*
[3]*Department of Physics, University of Surrey, Guildford, GU2 5XH, United Kingdom*
[4]*AECL Research, Chalk River Laboratories, Chalk River, Ontario, Canada KOJ 1JO*
[5]*Department of Physics, Australian National University, Canberra, Australia*
[6]*The Royal Institute of Technology, Physics Department I, S-104 44 Stockholm, Sweden*

(Received 19 December 1997)

The odd-proton nuclei ^{127}Pr and ^{131}Pm have been investigated using the ^{96}Ru(^{35}Cl,$2p2n$) and ^{96}Ru(^{40}Ca,αp)/^{96}Ru(^{39}K,$2p2n$) reactions, respectively, at beam energies of 164, 180, and 186 MeV. States belonging to the yrast bands of ^{127}Pr and ^{131}Pm, which are interpreted as being based upon the $h_{11/2}[541]\frac{3}{2}^-$ proton configuration, have been observed from the $\frac{11}{2}^-$ band head to spin $\frac{47}{2}^-$. The properties of these two new structures are observed to be different to those of similar configurations in the heavier odd mass isotopes. The systematics of the band crossings in the $\pi h_{11/2}$ bands of the odd mass Pr and Pm isotopes are discussed and compared with extended total Routhian surface calculations. [S0556-2813(98)03505-5]

PACS number(s): 21.10.Re, 21.60.Ev, 23.20.Lv, 26.60.+j

I. INTRODUCTION

The neutron-deficient nuclei in the $A \simeq 130$ region are of particular interest as the neutrons and protons occupy the same high-j intruder orbitals (in this case the $h_{11/2}$ orbital). The proton Fermi surface is located in the low-Ω region of the $h_{11/2}$ shell, while for the neutrons it evolves from high-Ω to mid-Ω states with decreasing neutron number: $N=78$ to 70. The yrast bands in the odd Pr and Pm nuclei are built upon a decoupled $h_{11/2}$ proton [1] and consequently the first $h_{11/2}$ proton alignment, predicted by standard cranked shell model (CSM) [2] calculations to occur at $\hbar\omega \simeq 0.3$–0.35 MeV, is Pauli blocked. Rapid increases in dynamic moments of inertia ($\mathcal{J}^{(2)}$) of the $\pi h_{11/2}$ bands in the ^{137,135,133}Pm [3–6] and ^{133,131,129}Pr [7–12] nuclei, at $\hbar\omega \simeq 0.35$–0.45 MeV have been attributed to the alignment of the second and third $h_{11/2}$ protons. CSM calculations have been used to interpret additional variations in the dynamic moment of inertia of the $\pi h_{11/2}$ bands in ^{137}Pm [3] and ^{131}Pr [9] at $\hbar\omega \sim 0.50$–0.6 MeV as resulting from the alignment of a pair of $h_{11/2}$ neutrons. In addition, for the previously known odd-mass Pr and Pm isotopes standard CSM calculations have been able to predict the correct magnitude of the experimentally observed alignment gain (Δi_x) for the $(\pi h_{11/2})^2$ crossing.

In the present work, we have extended the systematics of the odd praseodymium and promethium nuclei through a study of the most neutron-deficient isotopes populated to date: $^{127}_{59}Pr_{68}$ and $^{131}_{61}Pm_{70}$. From analysis of the data, it is observed that the gain in alignment at the first crossing for the two nuclei is considerably smaller than that predicted by standard CSM calculations. The apparent failure of the standard CSM in this instance has led us to reinvestigate the nature of the particle alignment in these odd-mass isotopes. This has been carried out by means of extended total Routhian surface (TRS) calculations [13].

Previous calculations have either treated the pairing interaction self-consistently, with a fixed value for the deformation, or conversely have modeled a given pairing gap with self-consistent deformation [14,15]. In the extended TRS calculations, both pairing and deformation are determined self-consistently. In addition, the pairing interaction contains both a monopole and a quadrupole force. Moreover, the time odd component of the quadrupole pairing field is found to be especially important in order to quantitatively describe the moments of inertia. Each configuration of a given parity and signature is minimized self-consistently, in addition, the state of the odd particle is blocked self-consistently, which is essential when describing crossing frequencies and polarization effects. This approach has been used successfully to describe the superdeformed bands of odd-A nuclei in the $A=190$ region [16] and intruder states in $A=110$ [13] mass region.

The extended TRS calculations for the nuclei ^{127}Pr and ^{131}Pm produce much better agreement with experimental results, both for extracted values of the dynamic moments of inertia $\mathcal{J}^{(2)}$ and spin alignment (i_x) than the standard cranked shell model. Furthermore, this model indicates that the proton contribution towards $\mathcal{J}^{(2)}$ and i_x for these light odd proton nuclei is considerably less than that from the $h_{11/2}$ neutrons, which is contrary to the predictions of previous standard CSM calculations. The present results indicate that in the most neutron-deficient odd-mass Pm and Pr nuclei the first alignment is primarily due to a pair of $h_{11/2}$ neutrons,

*Present address: Oliver Lodge Laboratory, University of Liverpool, Liverpool, L69 3BX, UK.
†Present address: Nuclear Science Division, Lawrence Berkeley National Laboratory, Berkeley, California.

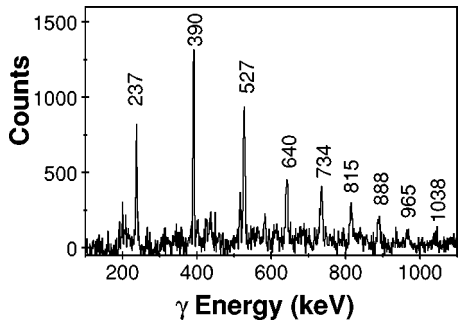

FIG. 1. Sum of the gates on the 237, 527, and 640 keV γ rays in ^{127}Pr from the ^{96}Ru+^{35}Cl reaction.

with only a small contribution from the $h_{11/2}$ protons. This suggests that the alignment process in these isotopes is somewhat more complicated than previously thought.

II. EXPERIMENTAL PROCEDURE

A. Population of ^{127}Pr

The odd-proton nucleus ^{127}Pr was populated using the ^{96}Ru(^{35}Cl,$2p2n$) reaction at a beam energy of 164 MeV, using the PEX (Pre Euroball Experiment) [17] array at the Neils Bohr Institute, Risø, Denmark. The array comprised four Compton suppressed bismuth-germanate (BGO) cluster detectors [18], each cluster housing seven (70–80 % efficient) hyperpure germanium detectors. The detectors were located at averaged angles of 105° and 165°, either side of the target position. Additional channel selection was achieved by use of a segmented silicon ball detector [19] for detection of evaporated charged particles, and a BaF_2 multiplicity filter. The target was comprised of two 250 μg/cm^2 highly enriched self-supporting ^{96}Ru metal foils. The typical beam intensity during the experiment was around 3–4 particle nA. Data were written to Exabyte tape and analyzed off-line by sorting the data into $4k\times4k$ particle-gated γ-γ coincidence matrices. Background-subtracted particle-gated spectra were then produced in order to construct a level scheme for the nucleus. Three γ rays of energies 237, 390, and 640 keV had been previously assigned to ^{127}Pr from a γ-recoil mass spectrometer (RMS) experiment [20,21]. In the present experiment, a $2p$ gated spectrum showed these same three γ rays. These transitions were not observed in $3p$ or αp gated spectra. This information, when combined with the RMS experiment, confirms that these γ rays belong to ^{127}Pr. Setting gates on these three γ rays on the $2p$ gated matrix (which contained approximately 8.4×10^6 events), produced the spectrum shown in Fig. 1. Gating on these same three γ rays in the $3p$ and αp mass gated spectra showed no evidence of any band structure, thereby confirming the assignment to ^{127}Pr. Systematics for the odd mass Pr nuclei suggest that this decoupled band is built upon the $h_{11/2}$ proton orbital. The particle gated matrices were found to contain too few statistics to enable directional correlation of oriented states (DCO) [22] analysis to be carried out. In the following discussion we have assumed that these transitions are stretched electric quadrupoles ($E2$'s).

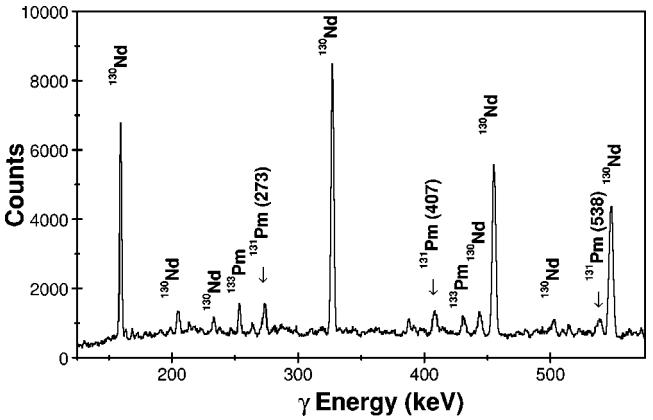

FIG. 2. Total projection for the αp gated matrix from the ^{96}Ru+^{40}Ca reaction with 2.4% of the total projection from the $3p$ (^{133}Pm) gated matrix removed. γ rays from the remaining channels are identified, the major contaminant remaining being ^{130}Nd.

B. Population of ^{131}Pm

The ^{131}Pm nucleus was populated using the ^{96}Ru(^{40}Ca,αp) and ^{96}Ru(^{39}K,$2p2n$) reactions at the TASCC facility at the Chalk River Laboratory, Canada. The target used was 500 μg/cm^2 of enriched ^{96}Ru on a 2 mg/cm^2 gold support. The gold was situated upstream of the target so that the beam passed through this first. The beam energy for the calcium reaction was 195 MeV before passing through the gold and approximately 180 MeV when incident upon the Ru target. In the potassium reaction the initial beam energy was 200 MeV, which corresponds to ~186 MeV when incident on the target. γ rays were detected using the 8π detector array [23] which has two distinct parts; the outer array houses 20 Compton-suppressed HPGe detectors (~25% efficient) and the inner array consists of 71 BGO scintillation detectors, providing sum energy (H) and fold (K) information. The 8π array was used in conjunction with a 4π modular array of Cesium iodide detectors, collectively known as the ALF miniball [24], which allowed for charged-particle identification and thus accurate reaction channel selection. Data were written to Exabyte tape for off-line analysis. During this analysis it was possible to set gates on the sum energy and/or fold so as to enhance reaction channels of interest. In the present experiment, tests showed that gates on H were slightly better than gates on K for differentiating between 2, 3, and 4 particle reaction channels. In off-line sorting, a high value of H was chosen for the Ca reaction so as to enhance any possible two-particle output channels (e.g., ^{131}Pm, populated via the αp channel), at the expense of the three and four-particle reactions channels. A matrix was created with this high H cut and a demand made that there was 1α and $1p$ present in the ALF miniball. This matrix contained approximately 1.4×10^6 γ-γ coincident events. The resulting total projection predominantly contained ^{130}Nd($\alpha2p$) and ^{133}Pm($3p$) channels. A small fraction ($\simeq$2.4%) of the total projection from the $3p$ gated matrix was subtracted from this spectrum, so as to eliminate the contamination from the very strong ^{133}Pm channel; the resulting spectrum is shown in Fig. 2. It was evident that the majority of the previously unassigned γ rays, labeled ^{131}Pm in Fig. 2 were not coincident with any of those from ^{130}Nd or ^{129}Pr, nor were they coincident with any known bands in

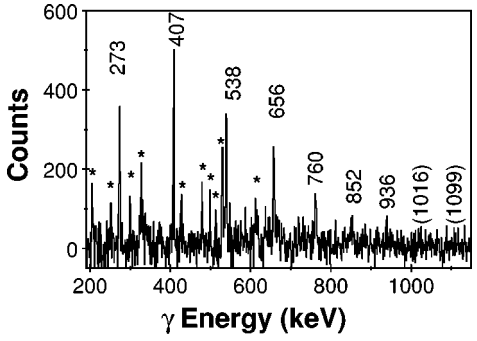

FIG. 3. Sum of the gates on the 273, 538, and 656 keV γ rays from the αp (high H) gated matrix observed from the ^{96}Ru+^{40}Ca reaction. Contaminants from ^{130}Nd are marked with an asterisk (see text for details).

other Pm or Pr nuclei. Gating on these transitions produced the new band shown in Fig. 3. This spectrum shows some evidence of contamination from ^{130}Nd, which arises solely as a result of using the 656 keV transition in the gate list. This is close to the 664 keV γ ray from band 1 in ^{130}Nd [25], which is populated via the αp channel, and results in significant broadening of the associated γ-ray transitions. Spectra gated on the 273 and 407 keV transitions show no evidence of this contamination. We therefore suggest that these newly observed transitions belong to the $\pi h_{11/2}$ yrast band of ^{131}Pm. It should be noted at this point that the same γ rays were also found to be present in the $2p$ gated matrix from the ^{39}K+^{96}Ru reaction. In this case, the ^{131}Pm is populated via the $2p2n$ reaction channel. This supports the present assignment of the band to ^{131}Pm. Once again DCO analysis was not possible for this band as the transitions were too weak and insufficient statistics were available. The cascade is therefore assumed to be composed of stretched electric quadrupole transitions.

III. EXPERIMENTAL RESULTS AND ANALYSIS OF DATA

From systematics we assign the new bands (Figs. 1 and 3) as the $\pi h_{11/2}$ yrast bands of ^{131}Pm and ^{127}Pr, respectively. Partial decay schemes for the nuclei ^{131}Pm and ^{127}Pr are shown in Figs. 4 and 5, respectively, alongside those for the yrast bands in the heavier Pm and Pr isotopes. The ordering of the γ rays in ^{131}Pm and ^{127}Pr has been deduced from the coincidence relationships between the γ rays and from the intensities of the observed transitions. An interesting feature of these data is that whilst the energy of the first transition in $\pi h_{11/2}$ bands of ^{127}Pr and ^{129}Pr remains essentially constant, in the case of ^{131,133}Pm, the $\frac{15}{2}^- \rightarrow \frac{11}{2}^-$ transition in the lightest isotope has a somewhat higher energy (273 keV as opposed to 252 keV). The next three transitions, however, in the ^{131}Pm band have a lower energy than equivalent γ rays in ^{133}Pm; a feature expected from systematics, since the quadrupole deformation is predicted to continue to increase as N decreases. These results suggest that the $\frac{15}{2}^-$ state in ^{131}Pm may be perturbed by the presence of an unseen state of the same spin and parity.

To compare experimental results with those derived from calculations, it is desirable to transform the results from the laboratory frame to the rotating nuclear frame. The usual

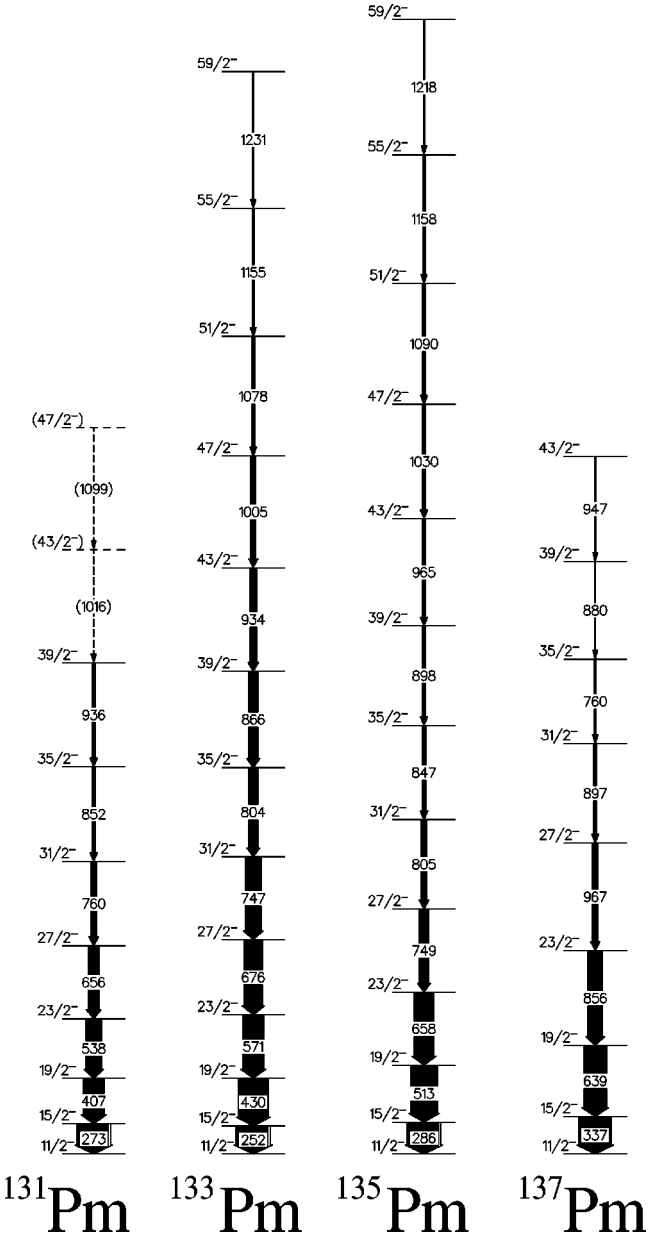

FIG. 4. Partial decay scheme for ^{131}Pm deduced from the present work. Also shown for comparison are the $\pi h_{11/2}$ yrast structures of ^{137,133,135}Pm. The data are taken from [3,4] (^{137}Pm), [4] (^{135}Pm), and [5,6,31] (^{133}Pm).

way of achieving this is to apply the methodology of Bengtsson and Frauendorf [26]. In the intrinsic frame of reference the quasiparticle aligned angular momentum (i_x) becomes

$$i_x = I_x(\omega) - I_{x,\mathrm{ref}}(\omega), \tag{1}$$

where I_x, the angular momentum on the rotation axis is given semiclassically as

$$I_x(\omega) = \sqrt{\left(I+\frac{1}{2}\right)^2 - K^2}, \tag{2}$$

and $I_{x,\mathrm{ref}}$ is a reference angular momentum found using the Harris formula [27]

$$I_{x,\mathrm{ref}}(\omega) = \omega \mathcal{J}_{\mathrm{ref}} = \omega(\mathcal{J}_0 + \omega^2 \mathcal{J}_1). \tag{3}$$

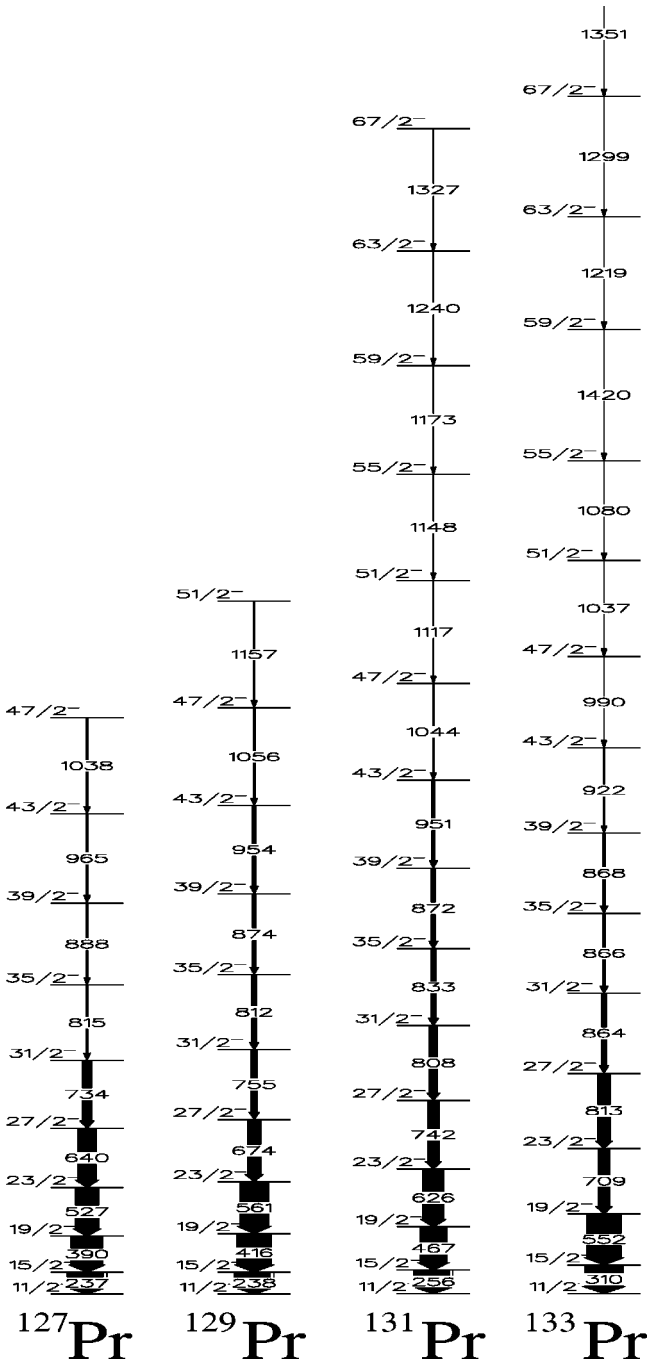

FIG. 5. Partial decay scheme for ^{127}Pr deduced from the present work. Also shown for comparison are the $\pi h_{11/2}$ yrast structures of ^{133,131,129}Pr. The data are taken from [7,8,32] (^{133}Pr), [10,11] (^{131}Pr), and [11] (^{129}Pr).

The Harris parameters used in the present work are, $\mathcal{J}_0 = 17.0\hbar$ MeV^{-1} and $\mathcal{J}_1 = 25.8\hbar^4$ MeV^{-3}. These values were originally derived from fitting transitions above the first band crossing in the yrast structure of ^{130}Ce [28].

Figures 6 and 7 show the dynamic moments of inertia ($\mathcal{J}^{(2)} = 4\hbar^2/\Delta E_\gamma$), and alignments for the yrast bands of the odd Pm and Pr isotopes, respectively, as a function of rotational frequency; the different behavior of the newly observed ^{131}Pm and ^{127}Pr is clearly evident. The rise in the $\mathcal{J}^{(2)}$, seen to occur at around $\hbar\omega \sim 0.35$–0.40 MeV for ^{135,133}Pm and $^{129-133}$Pr, is indicative of a band crossing.

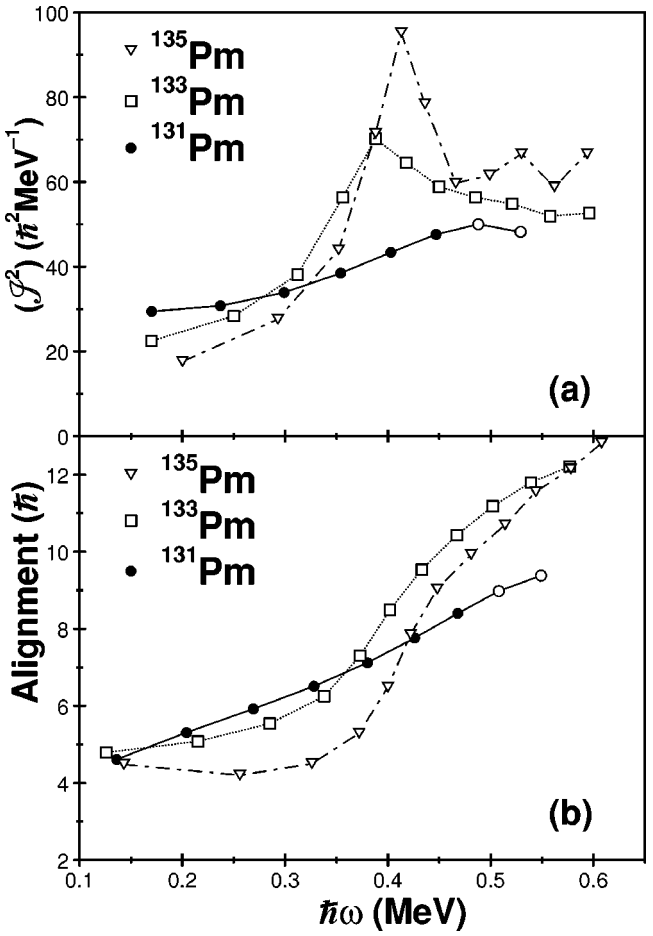

FIG. 6. (a) Dynamic moment of inertia ($\mathcal{J}^{(2)}$) as a function of rotational frequency for the $\pi h_{11/2}$ yrast bands of ^{131,133,135}Pm. (b) Alignment as a function of rotational frequency for the $\pi h_{11/2}$ yrast bands of ^{131,133,135}Pm. Tentative transitions in ^{131}Pm are shown in open circles.

This has been previously attributed to the alignment of a pair of $h_{11/2}$ protons from comparison with standard CSM calculations. In the lighter nuclei, this hump is spread out over several states indicating the presence of a strong interaction [29]. A strong interaction is also predicted by standard cranking calculations to occur in the $h_{11/2}$ bands of ^{131}Pm and ^{127}Pr. On extracting the alignment gain for the ^{131}Pm and ^{127}Pr $\pi h_{11/2}$ bands, we find that the experimentally derived value is of the order of 1.5–2.0$\hbar$, which is significantly less than the 5 to 6$\hbar$ predicted by the standard CSM calculations. If the proton pairing is reduced in the standard CSM calculations then the alignment gain seen experimentally can be reproduced. However, the pairing has to be reduced to unrealistically low levels in order to achieve this (e.g., $\Delta_p \sim 0.20$ MeV). An alternative approach was therefore required for an explanation of this discrepancy in the alignment gain. The self-consistent TRS was found to give much better agreement (see below) in the very neutron deficient nuclei. Thus, the next logical progression was to see how well the extended TRS calculations compared with experimental results for heavier Pm and Pr isotopes. Once again, the self-consistent model was found to provide a good agreement, but raised some interesting points.

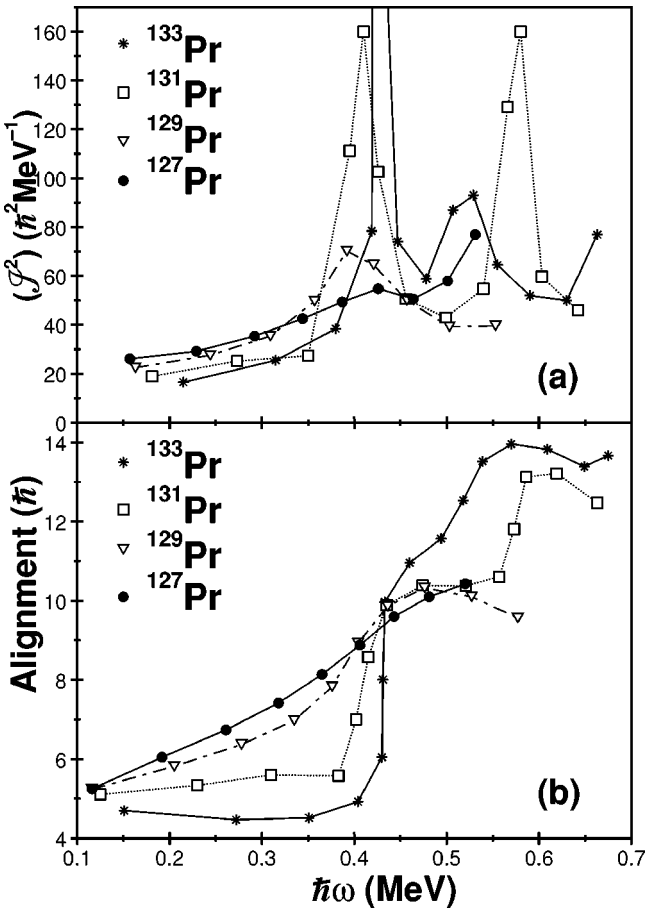

FIG. 7. (a) Dynamic moments of inertia ($\mathcal{J}^{(2)}$) as a function of rotational frequency for the $\pi h_{11/2}$ yrast bands in ^{127,129,131,133}Pr. (b) Alignment as a function of rotational frequency for the $\pi h_{11/2}$ yrast bands in ^{127,129,131,133}Pr.

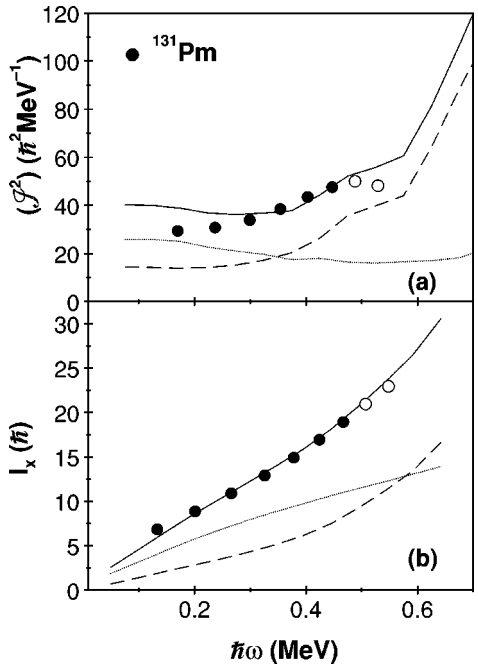

FIG. 8. (a) Dynamic moments of inertia as a function of rotational frequency for the $\pi h_{11/2}$ band in ^{131}Pm. The experimental values are represented by the dots. Theoretical values from the neutrons are shown as the dashed line, protons as dotted. The overall contribution from the neutrons and protons is shown as the solid line. The alignment of the $\nu g_{7/2}$ neutrons at around $\hbar\omega \simeq 0.8$ MeV is clearly visible. (b) Alignment gain as a function of rotational frequency of the $h_{11/2}$ yrast band of ^{131}Pm. The symbols and lines have the same meaning as defined in (a).

IV. DISCUSSION OF RESULTS

The data for ^{131}Pm show quite different characteristics in the variation of alignment and dynamic moment of inertia with rotational frequency compared to the heavier odd Pm nuclei. As Fig. 6(a) shows, the dynamic moment of inertia plot becomes much flatter for the lighter Pm nuclei. The alignment plot [Fig. 6(b)] supports this by showing no rapid increase at $\hbar\omega \sim$ 0.4 MeV. Standard CSM calculations, with $\beta_2 = 0.29$, $\gamma = -1°$, and $\Delta_P = 0.75$ MeV (values obtained from TRS calculations [30] for the $(\pi, \alpha) = (-, -\frac{1}{2})$ configuration in ^{131}Pm), predict an $h_{11/2}$ proton alignment at 0.45 MeV with 5–6$\hbar$ units of alignment gain. This clearly does not agree with the experimental results. A similar situation is predicted to occur in ^{127}Pr, and again is not observed in the experimental data, see Fig 7. However, when we compare results from the extended TRS calculations for both the ^{131}Pm and the ^{127}Pr$h_{11/2}$ bands, the shape of the dynamic moment of inertia plots and the value of i_x give much better agreement with experiment, see Figs. 8 and 9. These figures show the individual contributions made by the $h_{11/2}$ protons and neutrons and clearly indicate that in both cases the contribution to the $\mathcal{J}^{(2)}$ at $\hbar\omega \sim$0.4–0.5 MeV results primarily from the alignment of the $h_{11/2}$ neutrons. This feature is not reproduced by standard cranking calculations. In both nuclei the values of i_x are well reproduced.

Clearly, it is important to ensure that this self-consistent model can account for the behavior across a series of isotopes. When we apply the standard CSM to the heavier isotopes very good agreement is generally observed with the experimental results. These calculations predict the $h_{11/2}(FG)$ proton alignment to occur before the $h_{11/2}(ef)$ neutron alignment and this was the reason why the first alignment had been solely attributed to the $h_{11/2}$ protons [5]. As an example of the calculations, known data for ^{135}Pm are shown in Fig. 10 along with predictions from the latest self-consistent calculations. In this case, it is observed that there is an almost equal contribution from the protons and the neutrons at $\hbar\omega \sim$0.45–0.5 MeV, with the proton crossing occurring at the slightly higher frequency. Thus the previous suggestion that the alignment at this point was coming purely from the alignment of a pair of $h_{11/2}$ protons would appear to be too simple a picture. The calculations suggest that the alignment mechanism is not just derived from the protons on their own, but is in fact a far more subtle process.

On application of the self-consistent model to the $h_{11/2}$ band in ^{133}Pm, we once again observe a reduction in the contribution from the protons, this time to a greater extent than seen in ^{135}Pm, and again the alignment is predominantly $h_{11/2}$ neutron driven, with a small $(\pi h_{11/2})^2$ contribution. A systematic investigation of the data and the self-consistent model calculations shows an interesting effect,

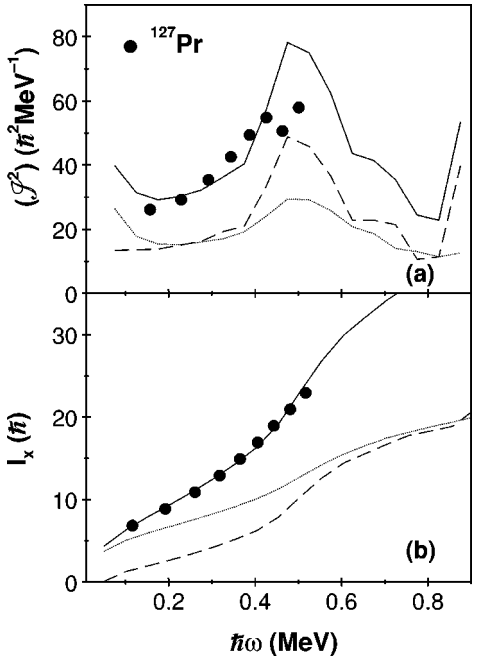

FIG. 9. (a) Dynamic moment of inertia as a function of rotational frequency for the $\pi h_{11/2}$ band in ^{127}Pr as a function of the rotational frequency. The experimental values are represented by the dots. Theoretical values from the neutrons are shown as the dashed line, protons as dotted. The overall contribution from the neutrons and protons is shown as the solid line. The theoretical calculations show an alignment occurring at $\simeq$0.5 MeV, which arises primarily from the alignment of a pair of $h_{11/2}$ neutrons. The $h_{11/2}$ proton alignment is not so heavily suppressed as in ^{131}Pm. The self-consistent cranked shell model calculations also indicate a $\nu g_{7/2}$ alignment occurring at $\simeq$0.9 MeV. (b) Alignment gain as a function of the rotational frequency for the $\pi h_{11/2}$ in ^{127}Pr. The symbols and lines have the same meaning as defined in (a).

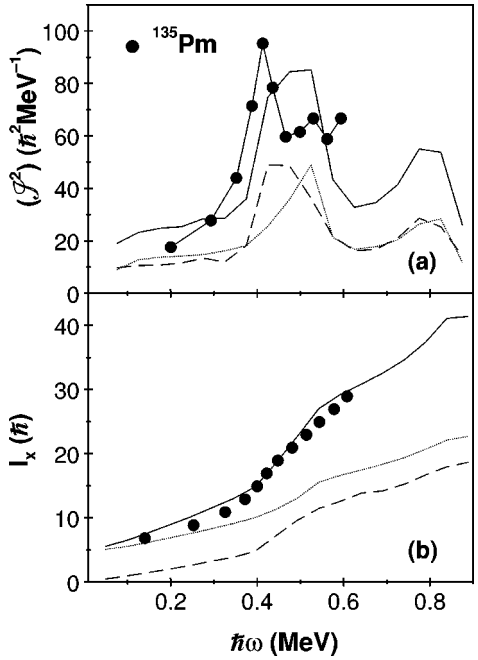

FIG. 10. (a) Dynamic moment of inertia as a function of rotational frequency for the $\pi h_{11/2}$ yrast band in ^{135}Pm. The experimental gain in $\mathcal{J}^{(2)}$ is well reproduced by the self-consistent model calculations. The symbols used for the calculations are the same as those defined in Figs. 7 and 8. In this heavier nucleus the gain in alignment is seen to arise from both $h_{11/2}$ protons and neutrons. A second alignment, which results from both pairs of $g_{7/2}$ neutrons and protons, is predicted to occur at around $\hbar\omega\simeq$0.8 MeV. (b) Alignment gain as a function of rotational frequency for the $\pi h_{11/2}$ band in ^{135}Pm. Again the individual contributions from the neutrons and protons is shown. The symbols and lines have the same meaning as defined in (a).

that is, that as the neutron number decreases, the contribution from the protons to the overall magnitude of the $\mathcal{J}^{(2)}$ decreases quite considerably, and the mechanism driving the alignment is derived primarily from the neutron contribution, Indeed the alignment of the $h_{11/2}$ protons is suppressed to such an extent that they have little or no effect at all in these very neutron-deficient isotopes. Similar effects are observed to occur in the odd Pr isotopes.

V. CONCLUSIONS

The negative-parity yrast states of the odd Pr and Pm nuclei result from the odd proton occupying a low-Ω $h_{11/2}$ orbital. In the present work, we have identified the negative parity yrast bands in ^{131}Pm and ^{127}Pr for the first time, observing them up to $\frac{47}{2}^-$. The properties of these two nuclei have been investigated and have been observed to differ from those of heavier odd-mass Pr and Pm isotopes and the predictions of the standard cranked shell model. In particular the gain in the spin alignment at $\hbar\omega\sim$0.40–0.45 MeV for the $h_{11/2}$ bands in ^{127}Pr and ^{131}Pm is far less than the standard CSM predicts. To further investigate this effect an extended cranked shell model has been used to explain the experimental results. This self-consistent cranked shell model has proved to give good agreement with the experimental results across a series of isotopes. Moreover, the results suggest that the alignment process at this frequency is much more complicated than previously thought. The self-consistent model has shown that for the two most neutron-deficient Pr and Pm isotopes the alignment of a pair of $h_{11/2}$ neutrons dominates over the alignment of an $h_{11/2}$ proton pair. However, as the mass increases in the odd A isotopes of Pm and Pr, the self-consistent model predicts that the alignment at $\hbar\omega\sim$0.40–0.45 MeV becomes increasingly dominated by the $h_{11/2}$ proton contribution, and that the $h_{11/2}$ neutron alignment gradually moves to higher rotational frequency.

The failure of the standard cranked shell model to explain certain features in this mass region, such as the nonobservation of an $h_{11/2}$ proton alignment in some of the bands seen in ^{133}Sm [5] has been previously discussed in terms of a residual n-p interaction. However studies have shown that the n-p effect, although present in several mass regions, is generally too small to explain all the observed discrepancies. More recent work [13] seems to suggest that it is the quadrupole-quadrupole pairing which plays the dominant role. Clearly more data are required on the very neutron-deficient isotopes in order to test our hypothesis.

ACKNOWLEDGMENTS

C.M.P would like to thank the University of York for supporting this research. A.J.B., C.C., D.T.J., and S.M.V. would like to acknowledge the support of EPSRC. We also wish to thank all the crews and technical support connected with the PEX array, Risø, Denmark, and at the TASSC facility, Chalk River, Canada. Thanks are also due to R. Darlington for manufacturing the targets used in both of the experiments and to J. Pfohl for providing data prior to publication on the Pm nuclei.

[1] M. J. Godfrey, P. J. Bishop, A. Kirwan, P. J. Nolan, D. J. Thornley, D. J. Unwin, D. J. G. Love, and A. H. Nelson, J. Phys. G **13**, 1165 (1987).
[2] R. Bengtsson and S. Frauendorf, Nucl. Phys. **A327**, 139 (1979).
[3] S. M. Mullins *et al.*, J. Phys. G **14**, 1373 (1988).
[4] C. W. Beausang, L. Hildingsson, E. S. Paul, W. F. Piel, P. K. Weng, N. Xu, and D. B. Fossan, Phys. Rev. C **36**, 602 (1987).
[5] P. H. Regan *et al.*, Nucl. Phys. **A533**, 476 (1991).
[6] A. Galindo-Uribarri, D. Ward, H. R. Andrews, G. C. Ball, D. C. Radford, and V. P. Janzen, Phys. Rev. C **54**, 1057 (1996).
[7] A. Goswami, S. Bhattacharya, M. Saha, and S. Sen, Phys. Rev. C **37**, 370 (1983).
[8] L. Hildingsson, C. W. Beausang, D. B. Fossan, and W. F. Piel, Phys. Rev. C **37**, 985 (1988).
[9] A. Galindo-Uribarri *et al.*, Report No. PR-TASCC-7: 3.1.28; AECL-11028, 1993 (unpublished).
[10] A. Galindo-Uribarri *et al.*, Phys. Rev. C **50**, R2655 (1994).
[11] P. K. Weng, P. F. Hua, S. G. Li, S. X. Wen, L. H. Zhu, L. K. Zhang, G. J. Yuan, G. S. Li, P. S. Yu, and C. X. Yang, Phys. Rev. C **47**, 1428 (1992).
[12] E. Dragulescu *et al.*, Rev. Roum. Phys. **T32**, 485 (1987).
[13] W. Satuła and R. Wyss, Phys. Scr. **T56**, 159 (1995).
[14] W. Nazarewicz, R. Wyss, and A. Johnson, Nucl. Phys. **A503**, 285 (1989).
[15] A. Granderath, P. Mantica, R. Bengtsson, P. Brentano, F. Seiffert, and R. Wyss, Nucl. Phys. **A597**, 427 (1996).
[16] R. Wyss and W. Satuła, Phys. Lett. B **351**, 393 (1995).
[17] R. Bark, EUROBALL Users Meeting, Padova, Italy, 1996 (unpublished).
[18] J. Eberth, Conference on Physics from Large γ-ray Detector Arrays, 1994 (unpublished), p. 160.
[19] T. Kuroyanagi, S. Mitarai, S. Suematsu, B. J. Min, H. Tomura, J. Mukai, T. Maeda, and R. Nakatani, Nucl. Instrum. Methods Phys. Res. A **316**, 289 (1992).
[20] J. Gizon *et al.*, Z. Phys. A **351**, 361 (1995).
[21] J. Genevey *et al.*, Inst. Phys. Conf. Ser. **132**, 671 (1992).
[22] D. Ward *et al.*, Nucl. Phys. **A529**, 315 (1991).
[23] H. R. Andrews *et al.*, Proposal for a National facility, Report No. AECL 8329, 1984 (unpublished).
[24] A. Galindo-Uribarri, Prog. Part. Nucl. Phys. **28**, 463 (1992).
[25] R. Wadsworth *et al.*, Z. Phys. A **333**, 411 (1989).
[26] R. Bengtsson and S. Frauendorf, Nucl. Phys. **A314**, 27 (1979).
[27] S. M. Harris, Phys. Rev. **138**, B509 (1965).
[28] D. M. Todd, R. Aryaeinajad, D. J. G. Love, A. H. Nelson, P. J. Nolan, P. J. Smith, and P. J. Twin, J. Phys. G **10**, 1407 (1984).
[29] M. J. A. de Voigt, Rev. Mod. Phys. **55**, 949 (1983).
[30] R. Wyss (private communication).
[31] J. Pfohl *et al.* (unpublished).
[32] E. S. Paul (private communication).